Journal of Magnetic Resonance 200 (2009) 349–353

Contents lists available at ScienceDirect

Journal of Magnetic Resonance

journal homepage: www.elsevier.com/locate/jmr

Communication

High Q calcium titanate cylindrical dielectric resonators for magnetic resonance microimaging

K. Haines [a], T. Neuberger [b], M. Lanagan [c], E. Semouchkina [c], A.G. Webb [d,*]

[a] Department of Electrical Engineering, Pennsylvania State University, University Park, PA, USA
[b] Huck Institute for Life Sciences, Pennsylvania State University, University Park, PA, USA
[c] Materials Research Laboratory, Pennsylvania State University, University Park, PA, USA
[d] C.J.Gorter Center for High Field MRI, Department of Radiology, C3-Q, Leiden University Medical Center, Albinusdreef 2, Leiden 2333 ZA, The Netherlands

ARTICLE INFO

Article history:
Received 16 May 2009
Revised 6 July 2009
Available online 14 July 2009

Keywords:
Dielectric
Ceramic
High frequency resonator
Microimaging

ABSTRACT

At high magnetic fields radiation losses, wavelength effects, self-resonance, and the high resistance of typical components all contribute to increased losses in conventional RF coil designs. High permittivity ceramic dielectric resonators create strong uniform magnetic fields in a compact structure at high frequencies and can potentially solve some of the challenges of high field coil design. In this study an NMR probe was constructed for operation at 600 MHz (14.1 T) using an inductively fed $CaTiO_3$ (relative permittivity of 156) cylindrical hollow bore dielectric resonator. The design has an unmatched Q value greater than 2000, and the electric field is largely confined to the dielectric itself, with near zero values in the hollow bore which accommodates the sample. Experimental and simulation mapping of the RF field show good agreement, with the ceramic resonator giving a pulse width approximately 25% less than a loop gap resonator of similar inner dimensions. High resolution images, with voxel dimensions less than 50 μm^3, have been acquired from fixed zebrafish samples, showing excellent delineation of several fine structures.

1. Introduction

Magnetic resonance microscopy is typically performed using vertical bore magnets with field strengths between 11.7 and 21.1 T. As the frequency increases, the design of efficient, low-loss resonators becomes increasingly challenging. Discrete component losses, reduced conductor skin depth and increased radiation losses are all effects which reduce the efficiency of conventional RF coils. For very small samples, high efficiency solenoidal coils can be used, but their high inductance limits their use for dimensions greater than a few millimeters, and the high electric field within the sample can cause heating in biological tissues. Lower efficiency transverse resonators such as the birdcage or millipede are difficult, though not impossible, to construct at small dimensions, and it is notable that only linear, rather than quadrature, versions of these coils are commercially available at small dimensions, presumably due to manufacturing difficulties.

As an alternative to these traditional designs, we recently proposed the use of high permittivity dielectrics for high field microimaging [1,2]. As described in detail, this work built upon designs that have been used for many years in electron paramagnetic resonance (EPR) [3–8]with operating frequencies well above 1 GHz. Dielectric resonators have also been used for larger scale MRI experiments [9], although this particular study used water, which has a very low Q value and high loss, as the dielectric material. In initial studies [1,2] the material used was barium strontium titanate, which had a very high relative permittivity of 323, but is relatively difficult to machine and to procure. Due to these and other manufacturing constraints, we previously used a two-disc arrangement with the sample placed between the two discs in a direction perpendicular to the long axis of the discs, which is not the optimal geometry in terms of available space for the sample or B_1 homogeneity. In this paper we have designed ceramic resonators from a material, calcium titanate, which is much more easy to machine, and is widely available at reasonable cost (<$100 per RF coil). By drilling a hole through the center of the cylindrical resonator the magnetic field distribution of the resonator is used more efficiently and larger samples, up to 4.5 mm in diameter, compared to the previous design can be investigated.

2. Materials and methods

A high relative permittivity material ensures both good energy storage and small dimensions at high frequencies. Calcium titanate ($CaTiO_3$) powder (Alfa Aesar, Ward Hill, MA), specified $\varepsilon_r = 156$,

* Corresponding author. Fax: +31 71 524 8256.
E-mail address: a.webb@lumc.nl (A.G. Webb).

1090-7807/$ - see front matter © 2009 Elsevier Inc. All rights reserved.
doi:10.1016/j.jmr.2009.07.012

was chosen for this reason as well as for its wide availability, low price ($70 per kg, each resonator requires ~175 g of powder) and ease of machining. The relative permittivity of the material was measured to be 156.3 using the Hakki–Coleman post resonant method [10] and network analyzer. The major dimensional constraint in terms of designing the dielectric resonators is the 8.9 cm diameter bore of the vertical 600 MHz (14.1 T) magnet, which is further restricted by the inside diameter of the gradients to 5.5 cm if imaging experiments are to be performed.

2.1. Electromagnetic simulations

Three-dimensional CST (Computer Simulation Technology, Darmstadt, Germany) Microwave Studio simulations were performed to determine the dimensions of the dielectric resonators as well as to model their electromagnetic properties. The resonator was simulated within a copper shielding tube of 5.5 cm diameter (representing the thin copper Faraday shield in the final MR probe), and a coaxial loop probe with waveguide port excitation was used to couple into the $TE_{01\delta}$ mode of the resonator. A single cylindrical dielectric resonator was modeled with a 4.8 mm diameter centrally-located hole directed along the horizontal axis of the resonator, as shown in Fig. 1(a), into which the sample is placed. It should be noted that this is a geometry perpendicular to the arrangement shown previously [1]: this new configuration orients the sample in a higher and more homogeneous RF field.

An inductive coupling loop for impedance matching was placed just outside the resonator, as also shown in Fig. 1(a). Time domain simulations were performed with the following parameters: relative permittivity 156, dielectric disc radius 2.325 cm and height 2.4 cm. Running a transient analysis yielded a resonance frequency of 602.4 MHz for the single cylindrical dielectric resonator. It should be noted that the effect of the Faraday shield is quite significant on the resonant frequency, which is about 80 MHz lower in free space.

2.2. Resonator construction and characterization

The starting material was $CaTiO_3$ powder, which was molded without an organic binder into a cylindrical shape using a 2.25 inch diameter die. Forming was completed using both an axial press (15,000 psi) and a cold isostatic press (25,000 psi). The resulting green samples were then sintered in a furnace at 1500 °C for 4 h. Initial testing showed that the powder had a lateral shrinkage of ~19% during sintering, and so the radius was made accordingly larger than the final desired dimension. Once sintered, holes were created in the ceramic discs using a 3/16 inch diameter diamond core drill. A diamond surface grinding wheel was used to achieve the final desired height which was fine-tuned through experimental S_{21} measurements with a network analyzer (Hewlett Packard HP8510C) using a standard two pickup-coil arrangement and a copper shielding tube identical to that used on the actual MR probe.

The quality factor (Q) of the sintered ceramic resonator was measured according to the technique described by Wakino et al. [11]. With the sample centered in a silver cavity, the S_{21} parameter on the network analyzer was measured. The resonant frequency of the $TE_{01\delta}$ mode was divided by the −3 dB bandwidth. Several samples were measured, and the results were averaged to give a Q value of 2081.

The fabricated resonator was placed within acrylic formers, and mounted in a cylindrical probe body, as shown in Fig. 1(b). Fine tuning of the resonators was accomplished by asymmetrically positioning small pieces of copper foil on both sides of the resonator faces as in the previous publications [1,2]. This effectively raised the resonant frequency to 600 MHz. Impedance matching was performed with a small wire loop of diameter 1.48 cm and variable series capacitor (1–30 pF, Johansson, Camarillo, CA) to achieve a 50 Ω match: the mutual coupling between the dielectric resonator and inductive loop is shown in Fig. 1(c). The unloaded Q was measured to be 1336 with a corresponding

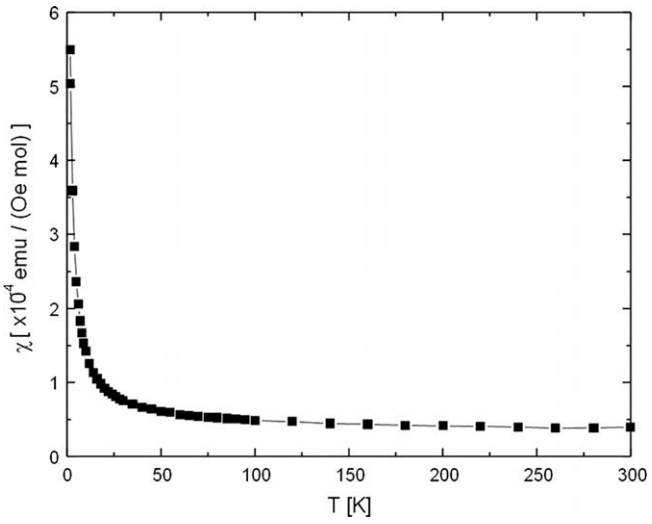

Fig. 2. Plot of magnetic susceptibility vs. temperature for $CaTiO_3$, showing the paramagnetic nature of the material.

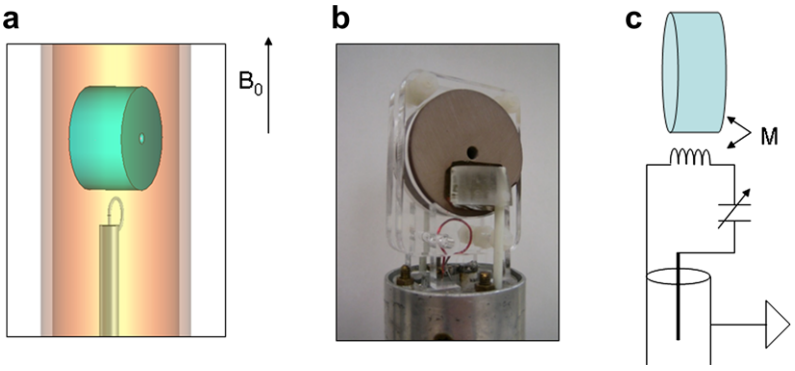

Fig. 1. (a) Schematic of the simulation setup for the cylindrical ceramic resonator, (b) photograph of the assembled probehead, (c) schematic showing the inductive feed with mutual inductance M used in combination with the variable capacitor to achieve a 50 Ω match.

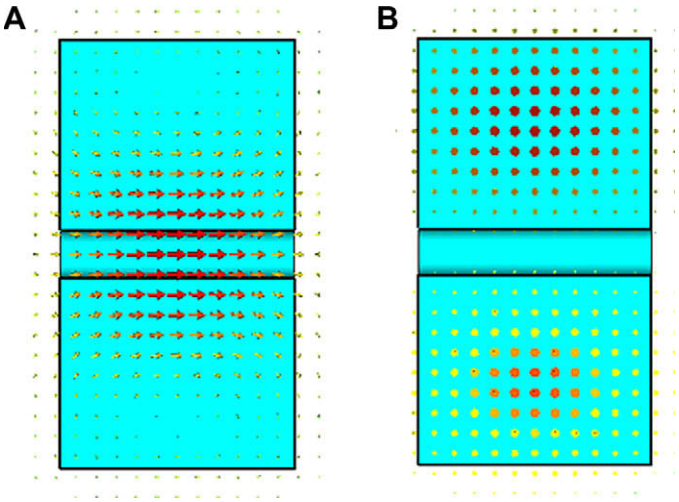

Fig. 3. (A) Simulated magnetic field distribution for the dielectric resonator. (B) Corresponding simulated electric field distribution.

−3 dB bandwidth of 449 kHz, approximately half that of the dielectric material itself.

A DC SQUID magnetometer was used to measure the magnetic susceptibility of a 117 mg sintered sample. The magnetic moment was measured over a temperature sweep from 0 to 300 K. Fig. 2 shows the resulting magnetic susceptibility normalized per mole of sample. The magnetic susceptibility is linearly related to temperature in the operating range of the current setup (15–20 °C). The value of the magnetic susceptibility is similar to that of other materials used in probe construction (Teflon, acrylic), and so is not expected to produce any significant image distortions. The cylindrical nature of the resonator also represents the optimum geometry for a homogeneous static magnetic field within the sample. The resonant frequency also shifts with temperature: experimentally we measured an increase of 4 MHz as the temperature varies from 12.8 to 19.7 °C. For this reason it is necessary to let the dielectric resonators thermally equilibrate within the experimental setup before starting any imaging experiments. No measurable frequency shift was seen during the MRI experiments.

2.3. Mapping the MR magnetic field

MRI experiments were performed using a Varian Direct Drive Console and a Magnex 14.1 T wide bore (89 mm) magnet. B_1 mapping measurements were performed using a three-dimensional spin–echo sequence on a sample of water doped with Gd-DTPA (T1 = 26 ms) using an incremental excitation pulse [12]. Fitting of the Fourier transformation of the acquired signal using the standard equation for the signal intensity of a spin-echo sequence produced a pixel-by-pixel estimate of the B_1 values.

2.4. MR microimaging

MRI experiments were performed on an ex vivo 6 week old zebrafish. After euthanizing the fish, it was fixed in a 4% formalin solution for 24 h. Prior to imaging, the fish was placed into a phosphate buffered saline (PBS) with a 2% v/v Gd-DPTA (Magnevist) solution for 2 days to shorten the relaxation times and thereby the total scan acquisition time: sodium azide was added as a biocide. The fish was then placed inside a 4 mm diameter glass tube of length 2 cm and filled with a perfluorinated liquid (FC43, 3M, MN) for the imaging experiment. The tube was centered within the dielectric resonator, and a 3D spin–echo sequence (TR/TE 250/20 ms, spatial resolution 47 × 42 × 42 μm, four signal averages, total scan time 1 h) was performed. Higher spatial resolution (20 × 20 × 25 μm) experiments were also performed, using 12 averages and took 16 h to acquire.

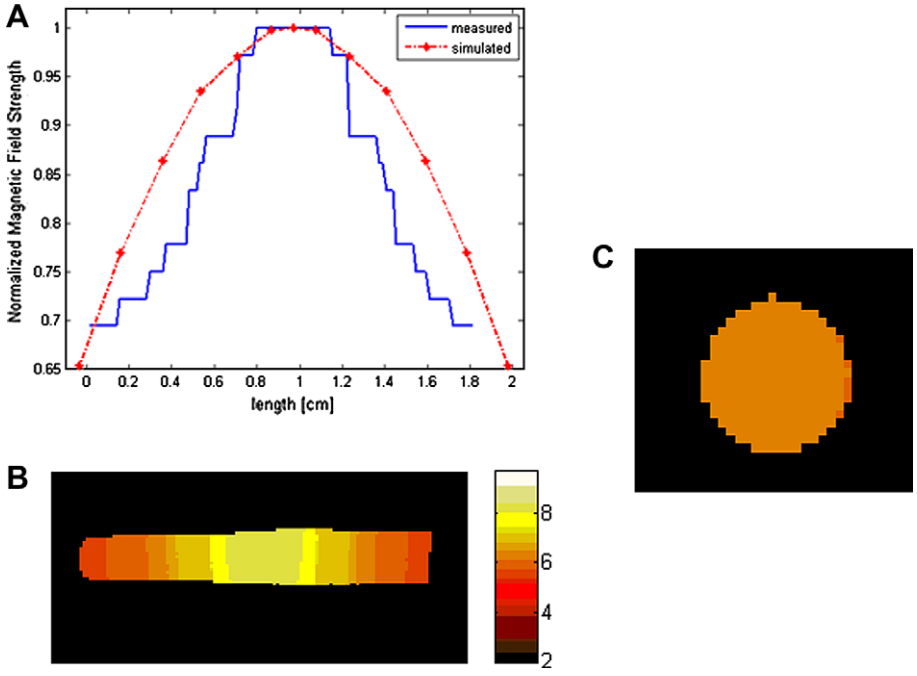

Fig. 4. (A) Comparison of simulated and experimental B_1 values along the length of the sample. The values are normalized to unity at the center of the resonator. (B) Central slice from the 3D B_1 map of the sample. The scale represents the B_1 field in microtesla. (C) An axial slice of the B_1 field through the sample: there is less than 5% variation across the sample.

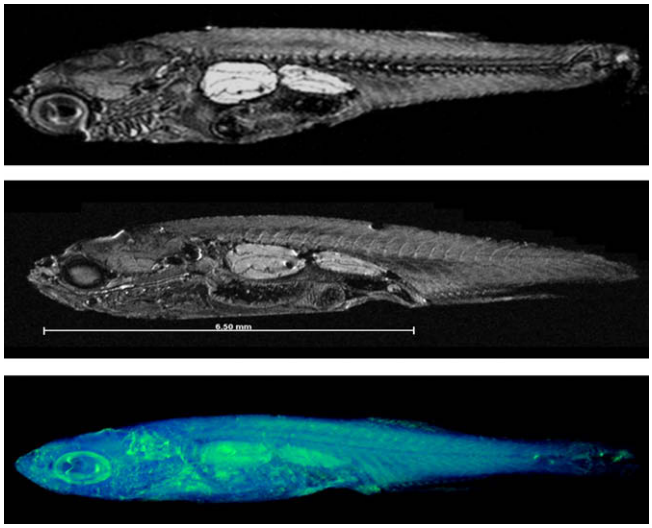

Fig. 5. (top) Single slice from a 3D data set acquired at a spatial resolution of $47 \times 42 \times 42$ μm. (middle) Single slice from a 3D data set acquired at a spatial resolution of $25 \times 20 \times 20$ μm. (bottom) Full 3D high resolution data set, volume rendered.

3. Results

3.1. Electromagnetic simulations

Fig. 3 shows the simulated magnetic and electric fields for the cylindrical dielectric resonator. As can be seen from the magnetic field distributions, the field is strongest along the axial center of the dielectric and reasonably homogeneous throughout the entire bore. From the electric field distributions it can be seen that the field is at a minimum along the principal axis of the cylinder. This is an advantage of the $TE_{01\delta}$ mode, since the sample is placed in the center of the cylinder, and so sample losses are minimized. It was noted that, from simulated data, the hollow bore configuration does not appreciably affect the distribution of the fields compared to a single solid cylinder. The simulated magnitudes of the magnetic field at the center of the dielectric configuration for a solid cylinder vs. a hollow cylinder differ only by about 5%. The introduction of a hollow bore to the dielectric cylinder also raises the resonant frequency of the $TE_{01\delta}$ mode by 2.4 MHz.

The measured B_1 maps for the cylindrical dielectric resonator are shown in Fig. 4. Line profiles along the major axes of the B_1 maps are plotted along with the corresponding CST simulated results. Field distributions along the equatorial plane of the resonator have also been measured and are homogenous to within 5% across the width of the sample (for the entire length of the resonator) of the dielectric resonator, as also shown in Fig. 4.

The 180° pulse widths for the dielectric resonator configurations was 30 μs giving a $B_1/\sqrt{P}$ of 294 $\mu T/\sqrt{Watts}$ (the power at the input of the probe was measured directly to account for losses from the cable from the amplifier and the transmit/receive switch). For comparison, a loop gap resonator was constructed with equal length and inner diameter to the dielectric resonator. The pulse width for this RF coil was approximately 25% larger than for the dielectric resonator.

3.2. Magnetic resonance imaging experiments

The zebrafish (Danio rerio) is an important model for developmental and genetic manipulation studies [13], since a large number of zebrafish mutations have been produced which mimic human disorders. Recently, high resolution MR microscopy has been used to provide high spatial resolution images of the adult zebrafish (at which point it is no longer optically transparent) both ex vivo and in vivo [14], as well as localized MR spectroscopy [15]. Here we use the ceramic resonator to acquire very high resolution three-dimensional datasets. Fig. 5 shows a series of individual slices and a surface rendering of the entire data set from the zebrafish. For the highest resolution data set, a number of different organs and structures can be visualized, as also shown in Fig. 6.

4. Discussion and conclusions

High permittivity ceramic resonators are compact, mechanically stable, high *Q*, low-loss devices that can be designed to be high sensitivity detectors for high field magnetic resonance. The magnetic susceptibility is similar to many plastics and other materials used for traditional RF coil design. The separation of electric and magnetic field components makes the design particularly suitable for lossy, biological samples. The dimensions of the resonator are determined by the dielectric constant of the material and the frequency of operation. Using commercially available materials, simple-to-design resonators have been shown here to already be useful at operating frequencies as low as 600 MHz. We anticipate that these types of resonator will become even more useful, and of course more compact, at higher frequencies such as the 900 MHz wide-bore microimaging system at the National High

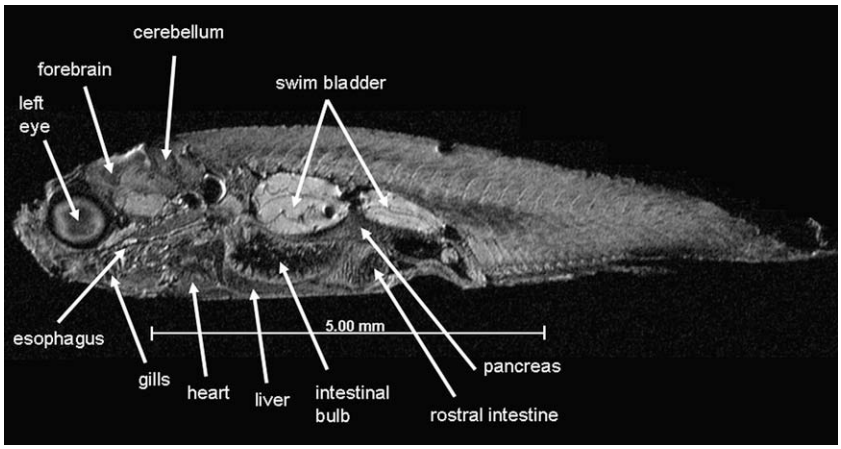

Fig. 6. Detailed mapping of structures and organs based upon the images acquired at a resolution of $25 \times 20 \times 20$ μm.

Magnetic Field Laboratory and planned next-generation 1.3 GHz magnets at a number of different institutions.

Acknowledgments

This work was funded in part by the Grace-Woodward Foundation at Penn State University. Dr. Keith Cheng of the Penn State College of Medicine is also gratefully acknowledged for supplying the zebrafish specimens.

References

[1] T. Neuberger, V. Tyagi, E. Semouchkina, M. Lanagan, A. Baker, K. Haines, A.G. Webb, Design of a ceramic dielectric resonator for NMR microimaging at 14.1 T, Concepts Magn. Reson. B Magn. Reson. Eng. 33B (2008) 109–114.
[2] V. Tyagi, E. Semouchkina, M. Lanagan, A. Baker, A. Webb, T. Neuberger, Ceramic Dielectric Resonators for High-Field Magnetic Resonance Imaging, in: IEEE Antennas and Propagation Society International Symposium, 2007, pp. 4316–4319.
[3] S.E. Bromberg, I.Y. Chan, Enhanced sensitivity for high-pressure Epr using dielectric resonators, Rev. Sci. Instrum. 63 (1992) 3670–3673.
[4] R.W. Dykstra, G.D. Markham, A dielectric sample resonator design for enhanced sensitivity of electron-paramagnetic-res spectroscopy, J. Magn. Reson. 69 (1986) 350–355.
[5] M. Jaworski, A. Sienkiewicz, C.P. Scholes, Double-stacked dielectric resonator for sensitive EPR measurements, J. Magn. Reson. 124 (1997) 87–96.
[6] A. Sienkiewicz, K.B. Qu, C.P. Scholes, Dielectric resonator-based stopped-flow electron-paramagnetic-resonance, Rev. Sci. Instrum. 65 (1994) 68–74.
[7] W.M. Walsh, L.W. Rupp, Enhanced electron-spin-resonance sensitivity using a dielectric resonator, Rev. Sci. Instrum. 57 (1986) 2278–2279.
[8] G. Lassmann, P.P. Schmidt, W. Lubitz, An advanced EPR stopped-flow apparatus based on a dielectric ring resonator, J. Magn. Reson. 172 (2005) 312–323.
[9] H. Wen, F.A. Jaffer, T.J. Denison, S. Duewell, A.S. Chesnick, R.S. Balaban, The evaluation of dielectric resonators containing H_2O or D_2O as RF coils for high-field MR imaging and spectroscopy, J. Magn. Reson. Ser. B 110 (1996) 117–123.
[10] R.W. Hakki, P.D. Coleman, A dielectric resonator method of measuring inductive capacities in the millimeter range, IRE Trans. Microwave Theory Tech. 8 (1960) 402–410.
[11] K. Wakino, H. Tamura, H. Tanaka, Precise measurement method for high frequency dielectrics, in: IEEE 7th International Symposium on Applications of Ferroelectrics, 1990, pp. 3–8.
[12] S.L. Talagala, J. Gillen, Experimental-determination of 3-dimensional Rf magnetic-field distribution of Nmr coils, J. Magn. Reson. 94 (1991) 493–500.
[13] D.M. Langenau, L.I. Zon, The zebrafish: a new model of T-cell and thymic development, Nat. Rev. Immunol. 5 (2005) 307–317.
[14] S. Kabli, A. Alia, H.P. Spaink, F.J. Verbeek, H.J. De Groot, Magnetic resonance microscopy of the adult zebrafish, Zebrafish 3 (2006) 431–439.
[15] S. Kabli, H.P. Spaink, H.J. De Groot, A. Alia, In vivo metabolite profile of adult zebrafish brain obtained by high-resolution localized magnetic resonance spectroscopy, J. Magn. Reson. Imaging 29 (2009) 275–281.